Int. J. Heat Mass Transfer. Vol. 34, No. 6, pp. 1393–1406, 1991
Printed in Great Britain

0017–9310/91 $3.00+0.00

Analysis of tissue injury by burning: comparison of *in situ* and skin flap models

KENNETH R. DILLER
Biomedical Engineering Program, Department of Mechanical Engineering, The University of Texas at Austin, Austin, TX 78712, U.S.A.

and

LINDA J. HAYES
Texas Institute for Computational Mechanics, Department of Aerospace Engineering/Engineering Mechanics, The University of Texas at Austin, Austin, TX 78712, U.S.A.

(*Received* 16 *August* 1988 *and in final form* 3 *July* 1990)

Abstract—The transient temperature field created in skin during a surface burn is modeled using the finite element technique. The two physical systems which are simulated are *in situ* tissue and an experimental skin flap chamber which is implemented for burn studies. Local cumulative injury in the tissue is calculated using an Arrhenius type injury model. The analysis shows that the burn experiments conducted in the skin flap chamber at temperatures up to 70°C will produce thermal histories which are negligibly different from those for *in situ* tissue for insult durations of less than 15 s.

INTRODUCTION

THERMAL burns to the skin are a commonly encountered type of injury that is physically painful and may potentially involve life-threatening consequences. Innumerable studies have been conducted for many years on the burn wound and various therapeutic regimens for it. Most of this work is based on experimental investigations with a heavy dependence on empirical techniques. Measurement and control of the thermal history within the affected tissue is often limited to events defining the initial tissue temperature and the transient surface conditions. Thus, the actual, local history in the tissue which has been exposed to elevated temperatures and which leads to a given severity of injury is usually unknown for specific thermal protocols.

Analytical models have been developed to predict the level of burn injury that will be produced by a defined thermal insult, beginning with the pioneering work of Henriques and Moritz in 1947 [1]. They applied the one-dimensional heat diffusion equation to obtain an analytical expression for the temperature rise in a homogeneous tissue resulting from exposure to a step increase in the surface temperature. This model was designed to match the initial and surface conditions created in complementary experimental burn trials which were conducted on pigs and on themselves. In each trial the apparent severity of the wound was assessed in terms of first, second and third degree injuries, and trials having equi-injury potential were identified. The local transient temperature–time records calculated by the diffusion model were used to predict the degree of injury under the assumption that the wound process could be described by a simple first-order exponential rate equation according to the Arrhenius model. The frequency factor in the damage model and the activation energy were then adjusted to fit the injury predicted by the model to agree with that measured in the various experimental trials. The values obtained by Henriques and Moritz provided quite good agreement within the spectrum of their experimental data, and they have been widely used by other investigators over the past 40 years.

Numerous subsequent investigators have presented additional models based on the work of Henriques and Moritz, which have enabled a broader class of burn protocols to be addressed. Beuttner used analytical methods to look at the effect of radiant energy deposition in skin [2, 3], and Stoll introduced computational procedures to determine the injury resulting from convective and radiative exposure [4, 5]. She also conducted numerous experiments on herself to measure the relation between the level of pain and the intensity and duration of surface heating [6]. Her studies were of great practical use in the design of thermally protective garments [7].

Because living tissue is a non-isotropic, non-homogeneous, composite material having an often complex geometry, numerical methods have been quite useful in the simulation of burn processes. Finite difference methods have been used to compute the thermal injury distribution within laser irradiated skin by Mainster *et al.* [8], Takata *et al.* [9], and Preibe and Welch [10], and within skin exposed to a scalding liquid by Palla [11]. Recently we have applied the finite element technique to model skin burns, including the effects of tissue metabolism, internal distributed con-

NOMENCLATURE

A	frequency factor in the burn damage integral [s^{-1}]	t	time [s]
c	specific heat [$J\,kg^{-1}K^{-1}$]	T	temperature [K]
ΔE	activation energy for burn injury [$J\,kmol^{-1}$]	z	axial position [m].
h	convective film coefficient [$W\,m^{-2}K^{-1}$]	Greek symbols	
k	thermal conductivity [$W\,m^{-1}K^{-1}$]	ρ	density [$kg\,m^{-3}$]
Q_m	metabolic rate in tissue [$W\,m^{-3}$]	ω	blood perfusion rate in tissue [ml blood (ml tissue)$^{-1}$ s^{-1}]
r	radial position [m]	Ω	degree of injury function.
$\mathscr{R}$	universal gas constant [$J\,kmol^{-1}K^{-1}$]		

vection by blood perfusion, and specific and finite system geometry [12]. In one application the model was used to predict the efficacy of thermal intervention into the insult process by post-burn cooling, with the somewhat surprising conclusion that there is practically no energy-based effect to be derived [13]. This result apparently stands against the widespread anecdotal evidence that there is significant benefit accrued from the immediate cooling of burned tissue. However, recent experimental data is in support of the model conclusions [14], although there is accumulating evidence that there does indeed exist a rational biochemical (as distinguished from thermal) basis for the efficacy of post-burn cooling. For further information on the above studies, a more comprehensive review of the analysis of skin burns is available [15].

Verification of the burn injury models is of course dependent on the availability of experimental data obtained in a manner consistent with the assumptions and constraints of the injury model. Most investigators have followed the lead of Moritz and Henriques to conduct macroscopic scale trials in which the burn is evaluated according to clinically based criteria [16]. These studies have been most useful in developing an understanding of how manipulation of the environmental temperature and of the time of exposure interact to produce a given level of burn. For example, we have adopted them in our own work on the effect of post-burn cooling regimens on the gross manifestation of burn wounds [17]. Nevertheless, the temperature field that develops in the skin during a burn process is of microscopic dimensions, and the injury process occurs locally within that field. The total wound which must be treated clinically is thus the volumetric accumulation in three dimensions of the local injury phenomena. Therefore, by imaging and characterizing the burn at the microscopic scale, we present a rational experimental approach which will be complementary to data obtained from a numerical model.

In the past there have been many investigations of the effect of burning on the microvasculature, including the results of thermal intervention by immediate post-burn cooling [18, 19]. A major difficulty with these studies was that they were either not conducted on skin tissue, which has its own characteristic vascular function and thermal properties, or in many cases, they required the animal to be kept under deep anesthesia and limited the protocol to only short, acute trial periods.

Transparent skin flap chambers have been surgically implanted on skin folds since the 1940s to enable chronic study of the dermal circulation [20]. More recently the chamber design and technique has been improved [21] and adapted [22] for studies of microvascular function at moderately elevated temperatures [23]. We have initiated a series of experiments in which tissue temperatures are elevated into the range for which thermal burns occur [24–26]. This preparation allows the microcirculatory function to be followed in a single, normalized dermal vascular network for periods of days or even weeks, without introducing inherent transient modifications associated with the administration of anesthesia. In this procedure each animal is able to function as its own control. We have applied the technique to evaluate local modifications to vasoactive function [24] and extravasation rate and interstitial transport of fluorescent labeled macromolecules [25, 26].

Although the skin flap model offers obvious advantages in the experimental study of the burn injury phenomena, a question arises as to how accurately the thermal field in the chamber matches that which occurs *in situ* in skin for a given protocol of exposure time and applied temperature at the skin surface. Since it is not practicable or desirable to introduce invasively an array of thermal sensors having the required spatial resolution in the skin to measure the thermal field created, numerical modeling techniques can be applied to compare predicted thermal histories for skin in the chamber and *in situ*. By adopting this approach we hope to be able to determine quantitatively how accurately a burn executed in the chamber simulates an *in situ* burn.

In this paper we present a finite element analysis of the thermal injury process, emphasizing a comparison between contact burn protocols executed *in situ* and in the chamber. The objective is to determine whether

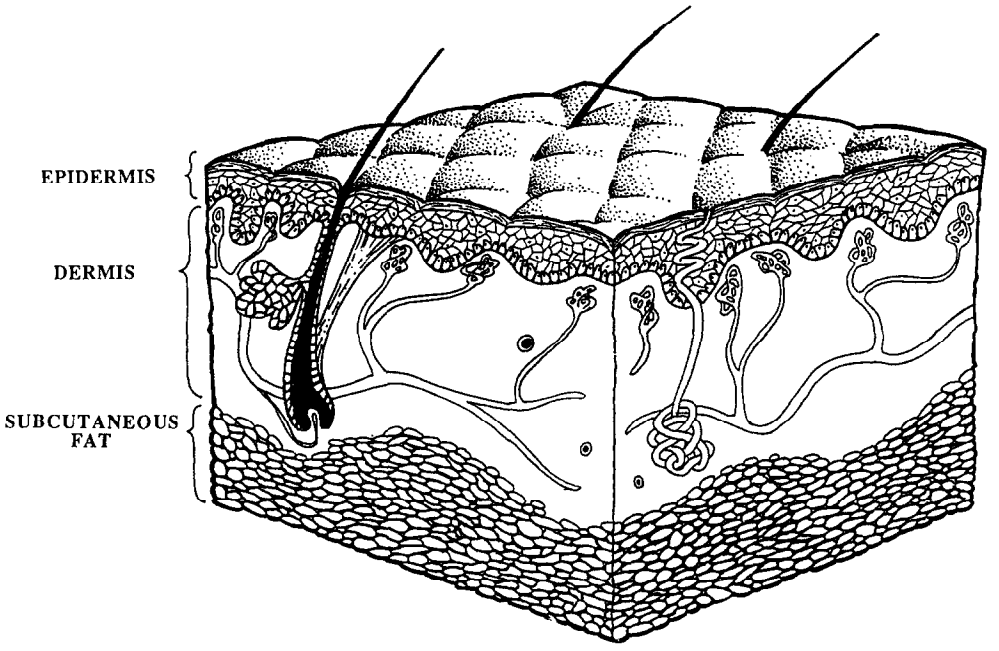

FIG. 1. Diagrammatic representation of the primary structural elements of the skin. A thin epidermis overlays a much thicker dermis having a diffuse vascular network, hair follicles and sweat ducts. Subcutaneous fat underlies the skin layers.

the range of thermal insult scenarios typically effected in the experimental model should produce a response that matches accurately the response produced by the identical scenario *in situ*. The most severe experimental wound that permits subsequent chronic measurement of physiological parameters occurs at a threshold temperature of about 70°C. Therefore, in the present study we have focused on describing a worst case for which a thermal insult was applied at 70°C to the skin surface for contact durations up to 30 s, although several experimental trials at higher temperatures were also evaluated. The threshold time is identified at which a substantial difference is noted between the experimental and *in situ* models. It is assumed that protocols at lower temperatures will elicit less of a differential between the two system responses. Numerical simulations are compared with transient temperature data for matching burn insult protocols executed in the skin flap chamber.

FINITE ELEMENT MODEL

Both the temperature and injury fields were computed by the finite element method [27, 28]. Grid networks were established to match the composite geometries of skin in the chamber and of a representative morphology *in situ*. A very simple representation of the physical structure of the skin is presented in Fig. 1, illustrating the parallel, layered arrangement of the component tissues and the diffuse vascular network within the dermis. As indicated, the vascular structure changes dramatically with distance from the surface, and regulation of blood flow through the microvascular network plays a key role in determining the temperature distribution within the skin.

The general vascular morphology of the skin has been studied extensively and is described in numerous references [29]. Blood flow enters at the base of the dermis through small arteries which branch into two or three layers of smaller vessels lying progressively closer to the surface. The top-most arteriolar plexus divides into many branches which become terminal capillary loops reaching up into the superficial papilla. These capillaries constitute the only nutritive flow component of the cutaneous circulation. The capillaries then collect in venular plexuses that increase in diameter with depth and match the arteriolar plexuses. At the deeper level where the larger vessels are found there may also exist arterio-venous anastomoses (AVA) which serve the function of regulating the relative degree of blood perfusion through the skin by shunting blood directly from the small arteries into the different subpapillary venous plexuses. The AVAs are thereby capable of effecting temperature regulation by varying the blood flow through the subpapillary vascular plexuses and the nutritional capillaries.

The vessels in the upper half of the dermis are so small that the blood in them is at thermal equilibrium with the surrounding tissue [30], whereas the larger vessels in the cutaneous plexus and the AVAs are able to support a significant temperature differential between the intravascular and extravascular spaces.

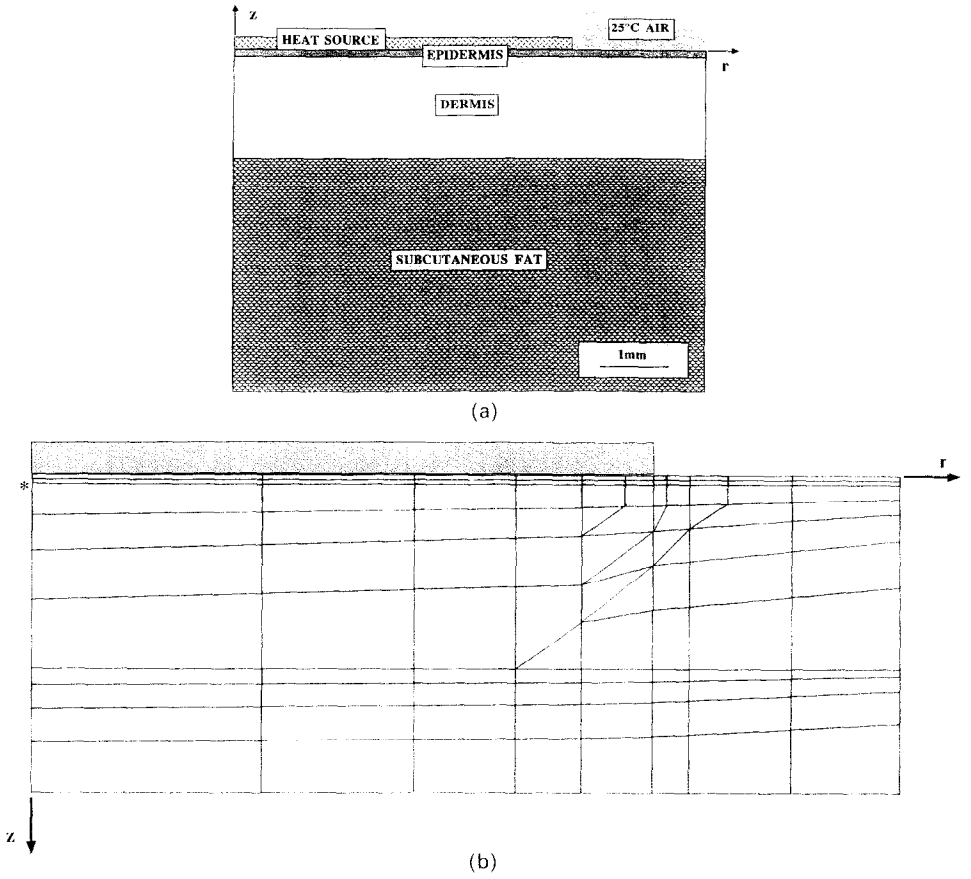

FIG. 2. (a) Geometry of *in situ* skin model in cylindrical coordinates. (b) Corresponding finite element grid.

Convective transport between blood flowing through these vessels and the surrounding tissue is proportional to the perfusion rate, which is minimal at low temperatures, of the order of 0.5 ml (min · 100 g) $^{-1}$ [31] and may increase considerably to more than 100 ml (min · 100 g) $^{-1}$ for temperatures in excess of 35 C. At high perfusion rates the amount of blood in the deep dermal plexuses may exceed that of the papillary capillaries by a factor of 30 [32], and in this condition local heat transfer in the skin may be dominated by convection with perfused blood rather than tissue conduction [33]. Thus, it is clear that a thermal model for the skin, especially at states of elevated temperature, must account for the effects of the spatial distribution of convective heat exchange with perfused blood.

The structure and function of the skin, the vascular network and the window chamber were prime considerations in laying out the finite element mesh for numerical modeling. The *in situ* and chamber grids were modeled using a cylindrically symmetric system in which the temperature was allowed to vary in the radial and axial coordinates. The geometries of the two systems with the corresponding grid meshes are shown in Figs. 2 and 3. The *in situ* model consists of an outer, thin layer of epidermis overlaying a much thicker dermis and subcutaneous fat. Blood perfusion and metabolism are assumed to occur only in the dermis as discussed above. The three materials of the composite tissue each have unique thermal properties as defined in the literature [34, 35] and are listed in Table 1. The geometry of the chamber model is shown in Fig. 3. The basic difference with the *in situ* model is that the subcutaneous fat is replaced with the chamber glass window of much thinner dimensions and different thermal properties.

A photograph of the chamber installed onto a dorsal skin flap of a hamster is shown in Fig. 4. When the chamber is surgically implanted onto the loose skin on the back of a hamster, all tissue is removed within the viewing aperture on one side of the fold, and the avascular underlying subcutaneous tissue is carefully dissected away on the other side. The chamber consists of a two-part frame with symmetric matching templates, with a central viewing opening that is mated together to support the flap for observation. A removable, protective window is installed on the template adjacent to the bottom side of the dermis, whereas the aperture in the template adjacent to the epidermal surface is left open to the environment. The burn is produced by contact between this surface and a heated medium, just as in the *in situ* case. The epidermis is prepared prior to surgery by shaving and application of a depilatory agent. Details

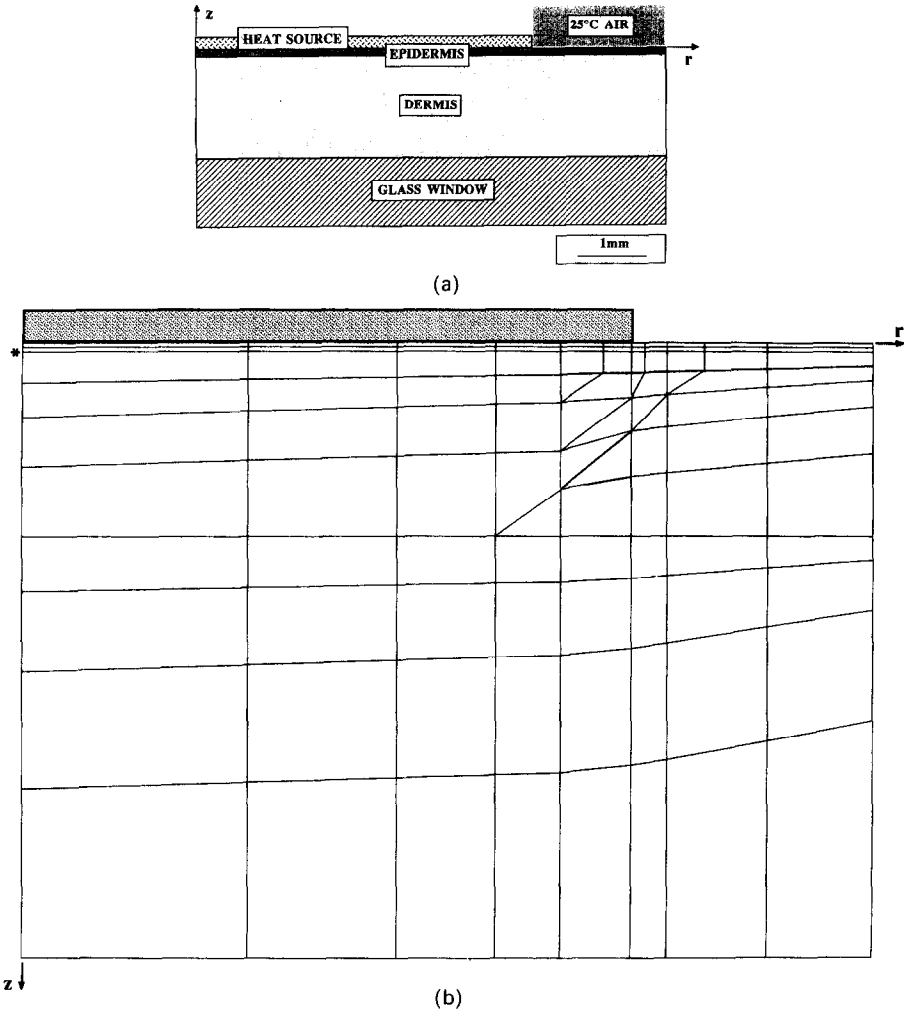

FIG. 3. (a) Geometry in cylindrical coordinates of skin within a surgically implanted transparent chamber. (b) Corresponding finite element grid.

of the chamber construction, use and implantation procedure have been presented previously [21].

The transient temperature field that develops in the skin as a result of exposure to a heated medium is described by the thermal diffusion equation, which includes the influence of tissue metabolism and blood flow. The resulting expression is called the 'bioheat equation' and has been the subject of recent rigorous analysis [36–38]. For our purposes we use the following format for the equation:

$$\rho c \frac{\partial T}{\partial t} = \nabla \cdot (k \nabla T) + Q_m + \omega_b \rho_b c_b (T - T_a). \quad (1)$$

The term on the left-hand side describes the energy storage within the tissue, and on the right-hand side of the equation the first term is the diffusion of heat, the second is distributed metabolic heat generation, and the third is convective heat exchange between blood flowing through the thermally significant vessels and the tissue, which is assumed to occur isotropically and homogeneously with respect to the spatial resolution of the analysis. Considerable debate has ensued over the physiological domains for which this assumption is valid [39–42]. The arguments for applying the bioheat equation are strongest for tissues having a vascular morphology similar to that of the skin, and it is reasonable to formulate the transient temperature distribution in the skin at elevated temperatures by equation (1) providing that the morphological and perfusion parameters are implemented properly. Quantitative values are listed in Table 1 for both the physical properties (k, thermal conductivity; c, specific heat; and ρ, density) and the physiological properties (ω_b, tissue blood perfusion; Q_m, tissue metabolism; and T_a, arterial blood temperature) which are used in equation (1).

Boundary and initial conditions for the present study are all specified as follows. Initially the entire system is assumed to be at a uniform temperature of 34°C. At time zero a planar heated substrate having a diameter of 5 mm is brought into perfect thermal contact with the skin surface and is held there for a specified period of time. Skin outlying the actively heated area is in thermal communication with the

Table 1. Parameter values used in the model

A	frequency factor in the damage integral	$3 \times 10^{10}\ s^{-1}$
c	specific heat:	
	skin	$4.0 \times 10^{3}\ J\ kg^{-1}\ K^{-1}$
	glass	$7.5 \times 10^{2}\ J\ kg^{-1}\ K^{-1}$
c_b	specific heat of blood	$3.3 \times 10^{3}\ J\ kg^{-1}\ K^{-1}$
ΔE	activation energy for burn injury	$6.3 \times 10^{8}\ J\ kmol^{-1}$
h	natural convection coefficient with air	$7\ W\ m^{-2}\ K^{-1}$
k	thermal conductivity:	
	epidermis	$2.1 \times 10^{-1}\ W\ m^{-1}\ K^{-1}$
	dermis	$3.7 \times 10^{-1}\ W\ m^{-1}\ K^{-1}$
	subcutaneous tissue	$1.6 \times 10^{-1}\ W\ m^{-1}\ K^{-1}$
	glass	$1.4\ W\ m^{-1}\ K^{-1}$
Q_m	metabolic heat generation	0
$\mathscr{R}$	universal gas constant	$8.314 \times 10^{3}\ J\ kmol^{-1}\ K^{-1}$
T_a	temperature of arterial blood	34 C
ρ	density:	
	skin	$1.04 \times 10^{3}\ kg\ m^{-3}$
	glass	$2.5 \times 10^{3}\ kg\ m^{-3}$
ρ_b	density of blood	$1.10 \times 10^{3}\ kg\ m^{-3}$
ω_b	blood perfusion rate:	
	epidermis	0
	dermis: papillary	0
	dermis: vascular plexuses	0 ml blood (min · 100 g tissue)$^{-1}$
		10^{0} ml blood (min · 100 g tissue)$^{-1}$
		10^{1} ml blood (min · 100 g tissue)$^{-1}$
		10^{2} ml blood (min · 100 g tissue)$^{-1}$
		10^{3} ml blood (min · 100 g tissue)$^{-1}$
		10^{4} ml blood (min · 100 g tissue)$^{-1}$
	subcutaneous tissue	0

environment via natural convection processes to an air environment at 25°C, as described by a film coefficient value, h, given in Table 1. The same coefficient is applied to characterize convection between the surface of the glass plate covering the dermis and the surrounding air. At the other radial boundaries the heat flow is assumed to be zero.

This boundary value problem is solved using a three-dimensional, axisymmetric transient finite element code [27] to obtain values for the temperatures in time and space, $T(r, z, t)$. The transient temperature data is then used to compute a local rate of injury formation at each node in the tissue. At each point in the grid the instantaneous temperature determines the injury rate according to the Arrhenius type function assumed for the process. The local rate of accumulation of injury, $d\Omega/dt$, is given by

$$\frac{d\Omega(r,z)}{dt} = A \exp\left\{-\frac{\Delta E}{\mathscr{R}T(r,z,t)}\right\}. \qquad (2)$$

Values for the frequency factor, A, and the activation energy, ΔE, are determined from empirical data, such as that of Henriques and Moritz [1]. Their values for these parameters were used for all simulations in this study and are given in Table 1. Alternate model parameter values may be applied which will yield substantially different injury predictions for high temperature burns [43]. Cumulative injury accrued over a specified time period at any location in the tissue is computed by integrating equation (2) in time

$$\Omega(r,z,t) = A\int_0^t \exp\left\{-\frac{\Delta E}{\mathscr{R}T(r,z,t)}\right\}dt. \qquad (3)$$

The local value of injury is represented in terms of the magnitude of the Ω function.

Henriques and Moritz [1] and other subsequent investigators have shown that the standard clinical classifications of burn injury severity are a non-linear function of Ω. Thus, a first degree wound corresponds to $\Omega = 0.53$, a second degree wound to $\Omega = 1.0$, and a third degree wound to $\Omega = 10^4$. These values represent threshold states that can be identified with clinical manifestations of injury. The model calculates a continuous distribution of injury within the tissue, and the threshold values can be used to build a map of profiles indicating the severity of the wound as it accrues.

EXPERIMENTAL MEASUREMENTS

A brief series of experiments was run to provide data for comparison with the finite element simulations. After installation of the skin flap chamber according to the standard protocol a hamster was prepared for a contact burn trial by deep anesthetization. A flat ribbon (of approximately 5 μm thickness) copper–constantan thermocouple was inserted between the bottom of the dermis and the adjacent

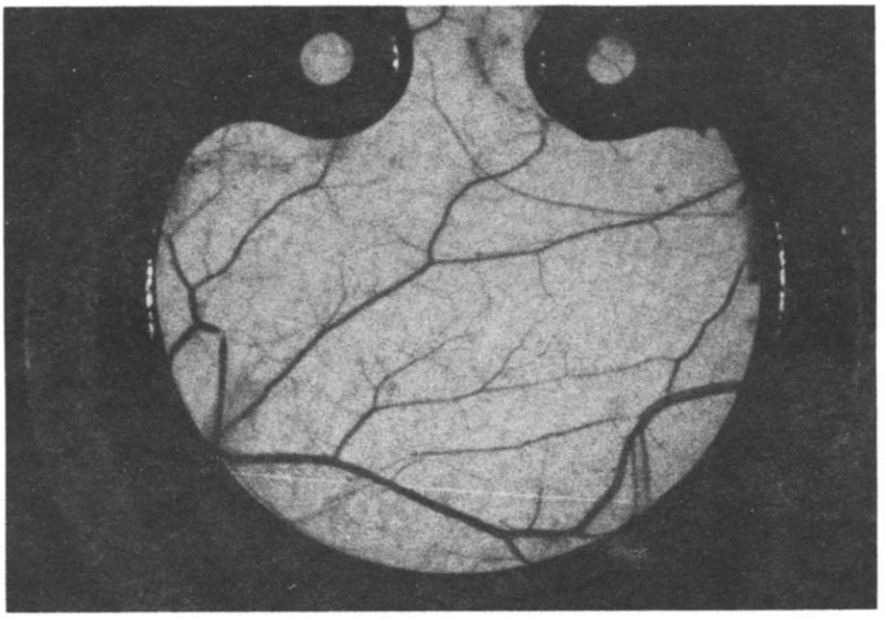

(a)

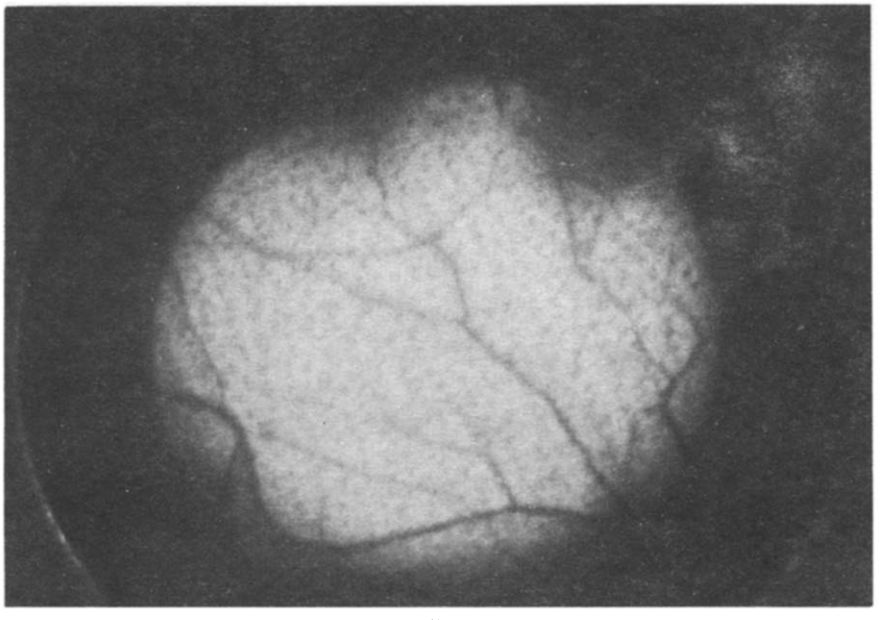

(b)

FIG. 4. A Syrian golden hamster with a transparent dorsal skin flap chamber installed. (a) Underside of the dermis, showing the larger elements of the vascular network which are visible through the center viewing aperture. A spring clip to hold the window in place to the frame is seen around the periphery of the image. (b) Exposed epidermis on the opposite side of the chamber having no covering window. Thermal boundary protocols are effected to the tissue on this surface of the skin. The total tissue thickness in the preparation is about 450 μm.

glass window of the chamber in order to monitor the thermal response to a surface burn at the deepest location within the tissue preparation. The epidermis was subjected to a contact burn from a heated metal substrate at either 70 or 90°C for either 5 or 10 s, and the temperature at the base of the dermis was monitored continuously until it had returned nearly to the initial value. Contact between the metal substrate and the tissue was initiated and terminated in a step-wise manner in order to most closely match the boundary conditions assumed in the numerical model.

RESULTS

In the past, the *in situ* tissue model has been used to investigate the injury produced for insult temperatures between 50 and 100°C and exposure times from 0.5 to 30 s [43]. In the present study the scope

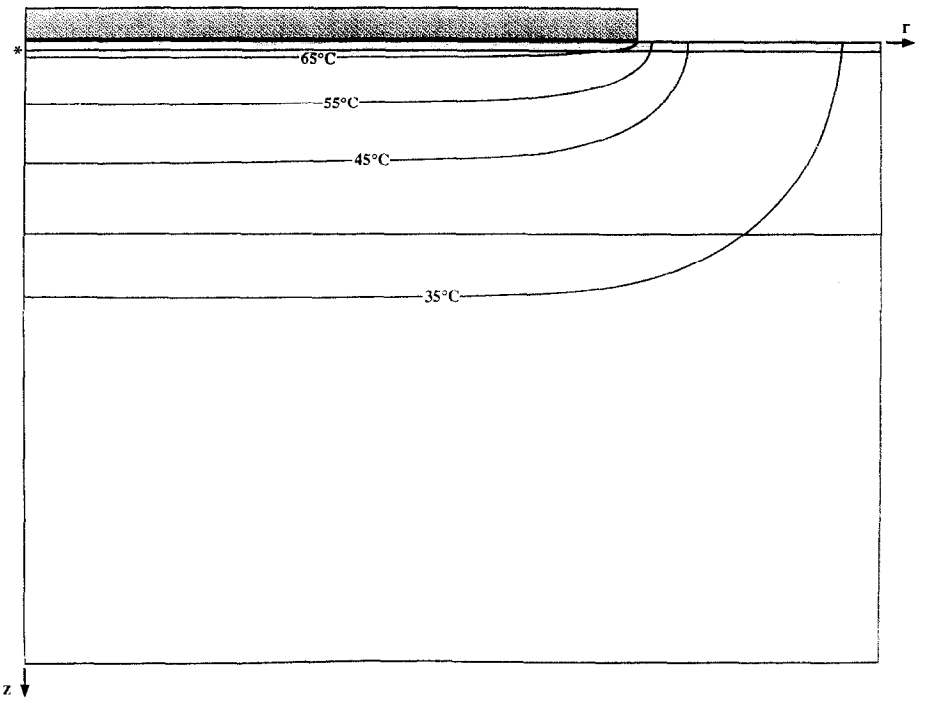

FIG. 5. Two-dimensional temperature field produced *in situ* owing to surface contact with a 70°C substrate for 4 s.

of burn protocols addressed is focused on a relatively small region of interest for experimental studies in the microcirculation of the skin flap chamber, namely for a 70°C insult temperature and for exposures between 0.5 and 30 s. Plots were produced from the solution of equations (1) and (3) illustrating the two-dimensional temperature and injury patterns, respectively, as they develop from the initiation of the burn process through removal of the heat source and cooling of the entire tissue surface by convection with environmental air.

Starting with an initially isothermal system, the temperature field builds with time to form a two-dimensional profile that penetrates into the tissue beneath the heating source. A typical thermal contour plot is illustrated for the *in situ* model in Fig. 5 for a 70°C burn, after 4 s have elapsed. Penetration of the temperature field into the tissue is obvious from the pattern of the isotherms. The time-wise progression of this process is shown in Fig. 6 in which the 50°C isotherm is followed for a 70°C, 30 s surface burn over the total course of the insult period. Movement of the isotherm into the interior of the tissue slows with time as a progressively greater depth into the tissue interior is achieved.

The local transient temperature histories which were calculated using the finite element model are applied in equation (3) to determine the pattern of injury produced during the burn process. Figure 7 shows the *in situ* isoinjury profiles at the end of the 70°C, 30 s burn, and Fig. 8 shows the advance of the second degree threshold injury into the skin during the actual burn process. In the present analysis the burn model parameter values identified by Moritz and Henriques [16] are used in equation (3) to perform the injury computations.

A primary objective of this investigation was to compare the thermal histories that could be expected in the skin chamber model and *in situ* and to identify the limiting severity of burn insult for which differences in the thermal histories and accrued injury were small. To this end the two numerical models were subjected to a series of identical thermal insult protocols, and the resulting temperature and injury contours were monitored and compared at incremental times. Figure 9 presents a comparison of the temperature profiles obtained for the two simulated systems as they evolved during the 70°C, 30 s burn procedure. Data for the *in situ* model are represented by solid lines and data for the chamber are represented by dashed lines. All of the data are plotted on the skin chamber grid for purposes of evaluating local differences in temperature. The 45°C isotherm represents the near threshold conditions for effecting thermal damage to living tissue, whereas at 60°C the rate of injury is significantly higher. The data clearly show that for exposure times as long as 4 s there is no discernible difference between the thermal histories in the two systems, and even at 8 s the differences are quite small. Major deviations occur only after 15 s when the 45°C profile has penetrated to the rear surface of the glass window, which is assumed to be insulated. At that position the temperature profiles assume quite divergent contours in order to enforce a

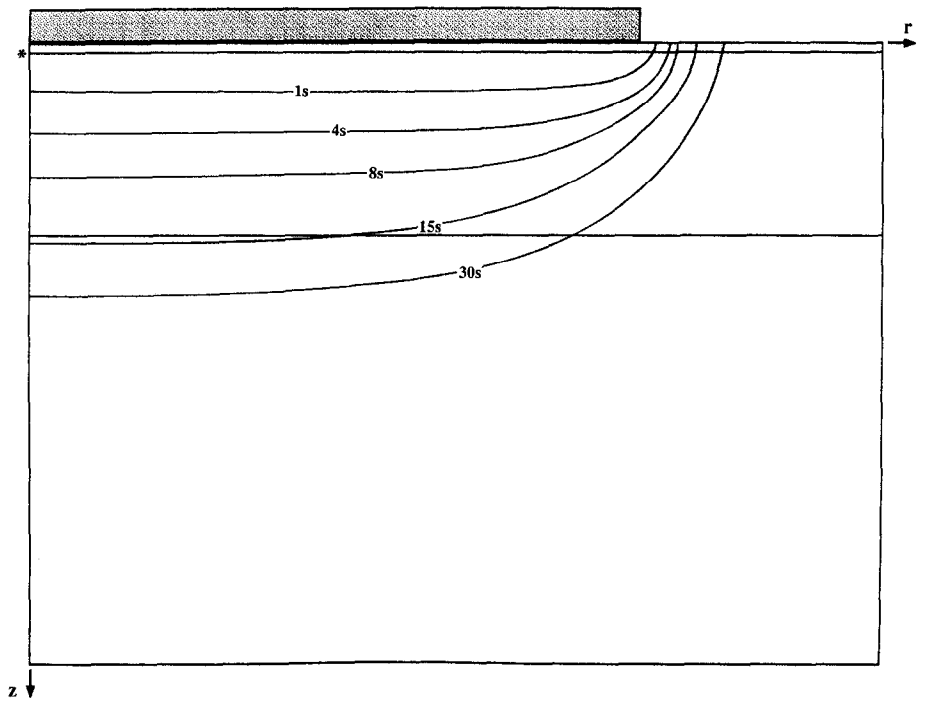

FIG. 6. Evolution of the 50°C isotherm *in situ* identified at the indicated times for a 70°C surface burn lasting 30 s.

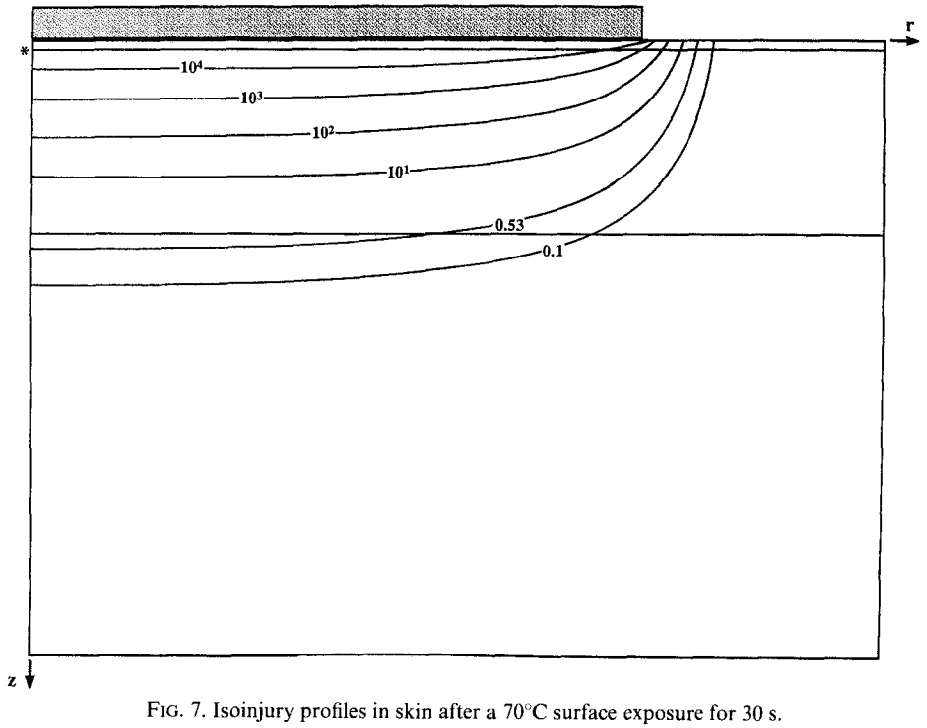

FIG. 7. Isoinjury profiles in skin after a 70°C surface exposure for 30 s.

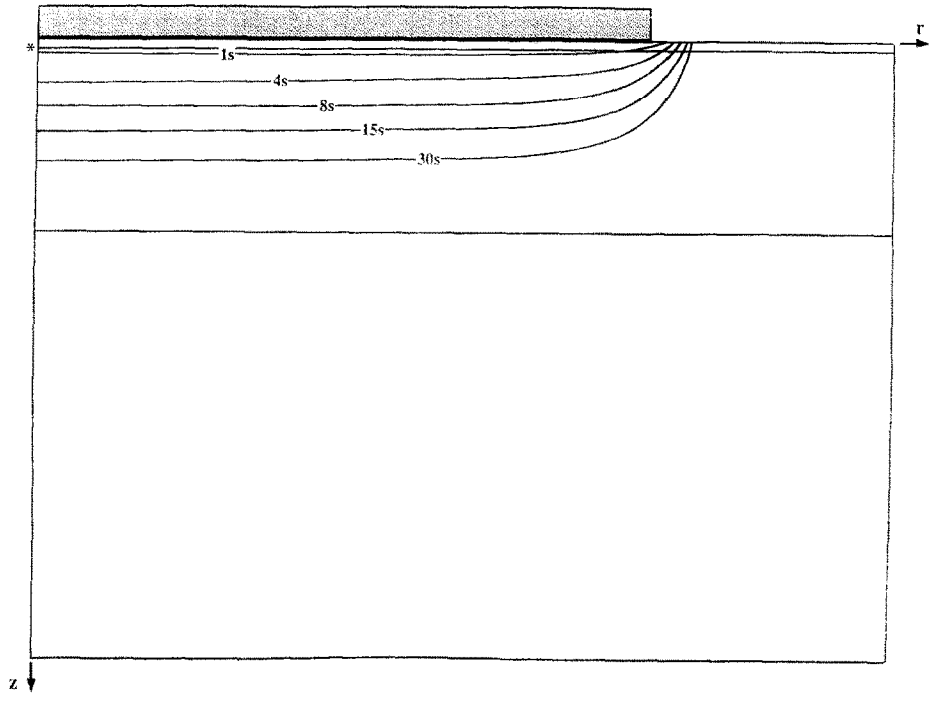

Fig. 8. Movement of the second degree injury profile through the skin at the indicated times.

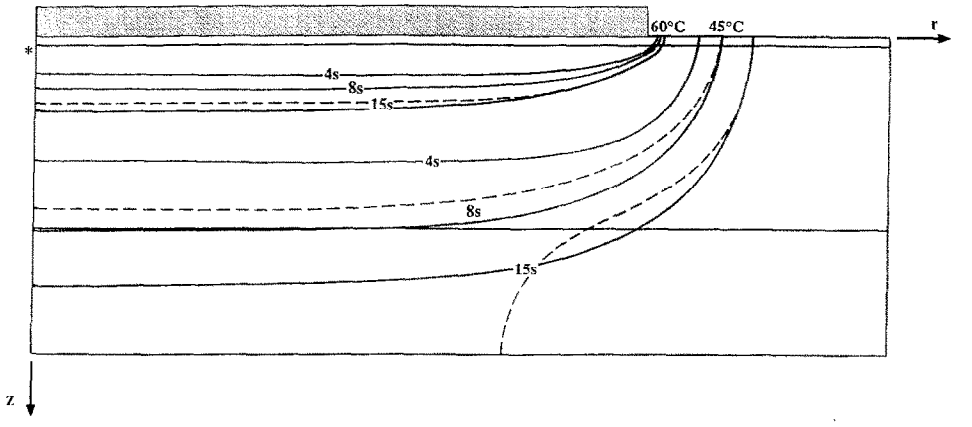

Fig. 9. Comparison of 45 and 60°C isotherms at the indicated times for identical surface burn protocols applied to the two model systems. *In situ* data is denoted by a solid line and skin chamber data which differs from *in situ* by a broken line. See the text for further details.

zero thermal gradient at the insulated window surface. However, since typical experimental protocols involve insult durations of only 3–5 s, the temperature field produced in the chamber should correspond very closely to that of *in situ* skin for an identical surface burn protocol.

The goal of this experimental program is to measure and evaluate physiological alterations to the skin and, in particular, to the microcirculatory function resulting from the inflammatory response induced by the burn injury. The skin flap chamber affords a convenient model for making the requisite observations, but a valid question is whether the thermal pattern effected in the chamber will produce the same degree of injury as would occur *in situ*. To address this issue Fig. 10 presents a direct comparison of the first and second degree injury contours as they penetrate into the tissue during the standard simulated burn scenario of Fig. 9. The first degree injury profiles are identical for the chamber and *in situ* models until the full 30 s of exposure is reached. At 8 s there is no discernible variation between the two models, and at 15 s the only difference is a reduced penetration of the second degree profile into the tissue in the *in situ* model. At the completion of the burn at 30 s both the first and second degree profiles are considerably different, as

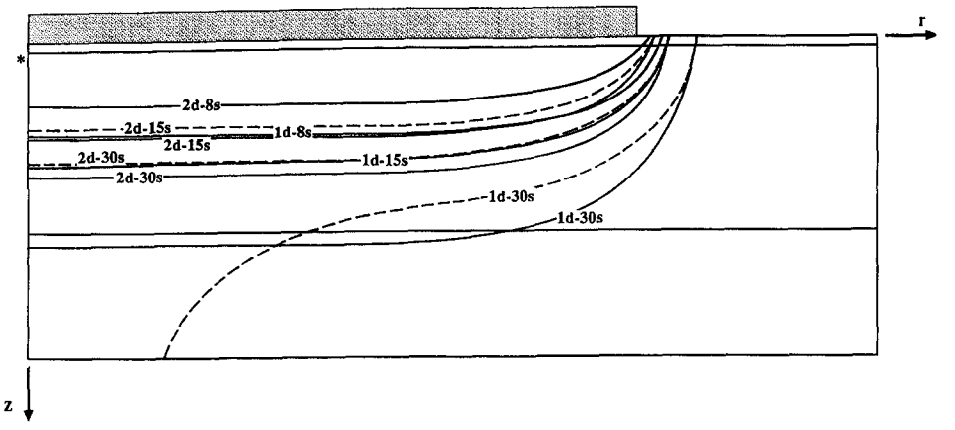

FIG. 10. Comparison of the penetration of the first (1d) degree and second (2d) degree injury contours during an identical burn scenario in the two skin models. Contours are plotted at the indicated times after start of the thermal insult on the skin surface. Notation corresponds to Fig. 9.

would be expected from the temperature patterns shown in Fig. 9. In particular, the first degree injury profile, which has reached the base of the cover glass, assumes a normal profile and moves outward from the center line of the chamber, following the general contour of the isotherms at that location. For contours not at the full chamber depth, the extent of penetration is reduced from that for *in situ* skin, due to the insulated surface assumed for the window.

The magnitude of blood perfusion in the skin is considered to play a major role in determining the local temperature [31, 32] as well as contributing significantly to total body thermal regulation [44, 45]. To this end a sensitivity analysis was performed to evaluate the influence of blood perfusion, which is assumed to be concentrated in the lower portion of the dermis and to be independent of the state of the system, on the transient temperature field during a burn. Simulations were performed for the standard 70°C burn at perfusion rates of 0, 10^0, 10^1, 10^2, 10^3 and 10^4 ml (min · 100 g)$^{-1}$ tissue. Figure 11 shows the 50°C isotherm contours obtained for the different perfusion rates after 4 s of burn insult on the epidermal surface. The 50° isotherm was selected for illustrative purposes because for this protocol it will penetrate into the tissue sufficiently to reach the perfused region deep into the dermis and because it is somewhat close to the threshold for which there will be significant accrual of injury. Figure 12 presents a corresponding plot of the second degree injury contours obtained for the various perfusion rates. The data indicate that as the perfusion rate increases there is a diminishing of the extent of penetration of the temperature field into the skin and of the total volume of injured tissue. Even though the perfusion is restricted to the lower level of dermis, these alterations are manifested well into the more superficial layers of the skin. The range of perfusion rates studied extends past the spectrum of physiologically realizable values; however, within the data shown there is a clear and consistent trend

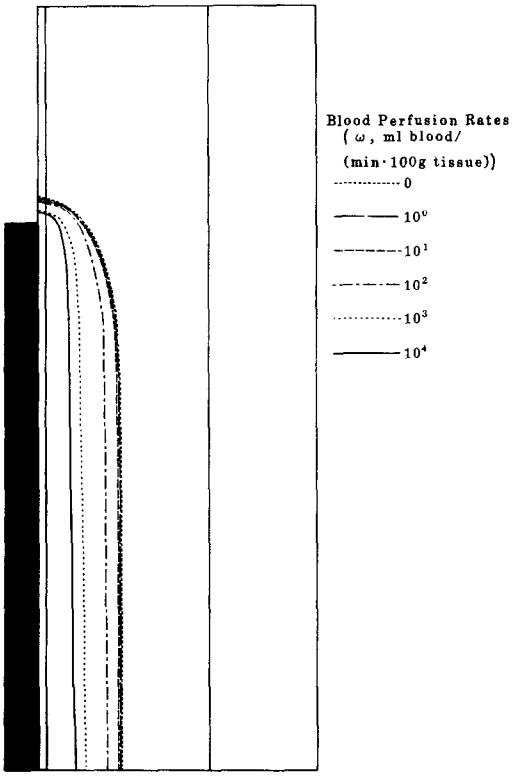

FIG. 11. 50°C isotherms calculated for blood perfusion through the lower half of the dermis at rates of 0, 10^0, 10^1, 10^2, 10^3 and 10^4 ml (min · 100 g)$^{-1}$ tissue at 4 s following the initiation of a 70°C surface burn.

toward cooling of the skin during a burn, thereby reducing the local degree of thermal injury.

The transient temperature profiles which were measured in the chamber at the base of the dermis for 70 and 90°C burns are shown in Fig. 13. The data is all self consistent and shows the expected decaying rates of rise and fall during the heating and cooling phases

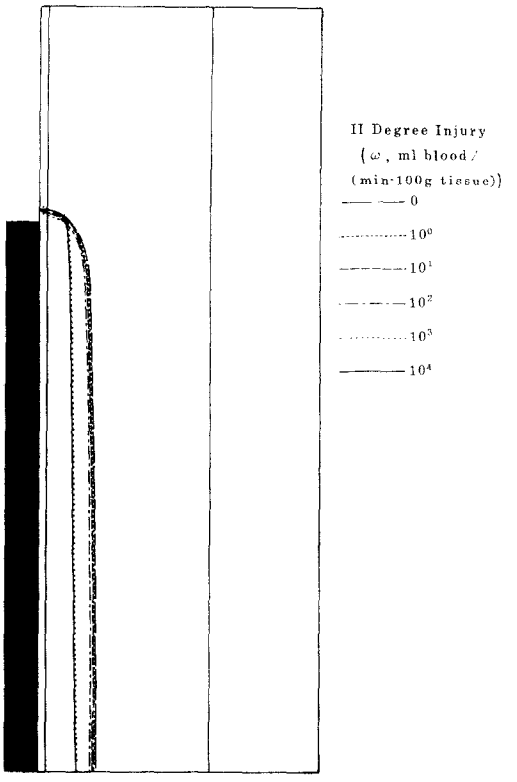

FIG. 12. Contours of second degree injury for the burn scenarios depicted for Fig. 11.

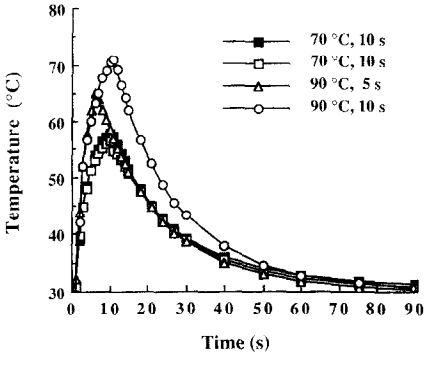

FIG. 13. Temperature histories measured at the base of the dermis for two burns at 70°C for 10 s, and two burns at 90°C, one for 5 s and one for 10 s, as indicated.

of the protocols. A temperature rise of approximately 2/3 of the differential between the initial and boundary values was achieved at the base of the dermis after 10 s of heating for both of the insult conditions.

The experimental data for the 70°C burn trials were compared with the results of the numerical simulation for the identical conditions as a verification of the model. The measured and simulated temperature histories are plotted together in Fig. 14. For this simulation it was assumed that the blood perfusion rate was 1 ml (min · 100 g)$^{-1}$, and the total thickness of the skin preparation was 500 μm. As expected, there

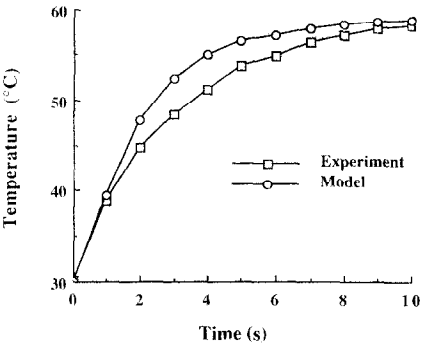

FIG. 14. Measured and simulated temperature histories at the interface of the dermis and the underlying glass window of the flap chamber.

is some variation in the thickness of the tissue in the observing aperture of the flap among the trial animals, with the general range of 400–500 μm.

Figure 14 demonstrates a very good agreement between the measured and simulated data sets. The model predicts a slightly higher rate of temperature rise under the simulated conditions, but there is not sufficient experimental evidence to justify modification of the simulation parameters, such as increasing the perfusion rate by one or two orders of magnitude to elicit a corresponding reduction in temperature, to tune it for a better match with the measured data. However, the degree of agreement between the model and the experiments is sufficient to provide an acceptable level of confidence in the numerical simulations.

CONCLUSIONS

These results indicate that for all practical purposes relating to the experimental protocol, which involves relatively short exposure times to elevated temperatures, there is no distinguishable difference between the extent of injury that should be expected for the skin flap chamber in comparison with *in situ* skin. Therefore, from a thermal perspective the dorsal skin flap chamber should be an acceptable experimental model for simulating and studying the effects of burn injury in the microcirculation, and the benefit of being able to observe the microvasculature in a chronic preparation both before and after a burn wound is not negated by any significant alteration of the injury pattern from that anticipated in a normal, unaltered tissue system.

Acknowledgement—This research was sponsored in part by N.I.H. Grant No. GM 21681. Dr Shanti Aggarwal and Joseph Yip assisted in obtaining temperature measurements for the burn protocols in the skin flap chamber.

REFERENCES

1. F. C. Henriques and A. R. Moritz, Studies of thermal injury, I. The conduction of heat to and through skin and the temperatures attained therein. A theoretical and

an experimental investigation, *Am. J. Pathol.* **23,** 531–549 (1947).
2. K. Beuttner, Effects of extreme heat and cold on human skin, I. Analysis of temperature changes caused by different kinds of heat application, *J. Appl. Physiol.* **3,** 691–702 (1951).
3. K. Beuttner, Effects of extreme heat and cold on human skin, II. Surface temperature, pain and heat conductivity in experiments with radiant heat, *J. Appl. Physiol.* **3,** 703–713 (1951).
4. A. M. Stoll, A computer solution for determination of thermal tissue damage integrals from experimental data, *Inst. Radio Engrs Trans. Med. Electron.* **7,** 355–358 (1960).
5. J. A. Weaver and A. M. Stoll, Mathematical model of skin exposed to thermal radiation, *Aerospace Med.* **40,** 24–30 (1969).
6. A. M. Stoll and M. A. Chianta, Burn production and prevention in convective and radiant heat transfer, *Aerospace Med.* **39,** 1097–1100 (1968).
7. A. M. Stoll and M. A. Chianta, Heat transfer through fabrics as related to thermal injury, *Ann. N.Y. Acad. Sci.* **33,** 649–670 (1971).
8. M. A. Mainster, T. J. White, J. H. Tips and P. W. Wilson, Transient thermal behavior in biological systems, *Bull. Math. Biophys.* **32,** 303–314 (1970).
9. A. N. Takata, L. Zaneveld and W. Richter, Laser-induced thermal damage of skin, SAM-TR-77-38, USAF School of Aerospace Medicine (1977).
10. L. A. Preibe and A. J. Welch, A dimensionless model for the calculation of temperature increase in biologic tissues exposed to nonionizing radiation, *IEEE Trans. Biomed. Engr* **BME-26,** 244–250 (1979).
11. R. L. Palla, A heat transfer analysis of a scald injury, Report No. NBSIR 81-2320, U.S. National Bureau of Standards (1981).
12. K. R. Diller and L. J. Hayes, A finite element model of burn injury in blood perfused skin, *Trans. ASME, J. Biomech. Engr* **105,** 300–307 (1983).
13. K. R. Diller, L. J. Hayes and C. R. Baxter, A mathematical model for the thermal efficacy of cooling therapy for burns, *J. Burn Care Rehabil.* **4,** 81–89 (1983).
14. O. P. Jakobsson and G. Arturson, The effect of prompt local cooling in oedema formation in scalded rat paws, *Burns* **12,** 8–15 (1985).
15. K. R. Diller, Analysis of skin burns. In *Heat Transfer in Medicine and Biology, Analysis and Applications* (Edited by A. Shitzer and R. C. Eberhart), Vol. 2, pp. 85–134. Plenum Press, New York (1985).
16. A. R. Moritz and F. C. Henriques, Studies of thermal injury, II. The relative importance of time and surface temperature in the causation of cutaneous burns, *Am. J. Pathol.* **23,** 695–720 (1947).
17. K. F. Thompson and K. R. Diller, Use of computer image analysis to quantify contraction of wound size in experimental burns, *J. Burn Care Rehabil.* **2,** 307–321 (1981).
18. M. P. Wiedeman and M. P. Brigham, The effects of cooling on the microvasculature after thermal injury, *Microvasc. Res.* **3,** 154–161 (1971).
19. D. C. Ross and K. R. Diller, Therapeutic effects of postburn cooling, *Trans. ASME, J. Biomech Engr* **100,** 149–152 (1978).
20. G. H. Algire, An adaptation of the transparent-chamber technique to the mouse, *J. Natn. Cancer Inst.* **4,** 1–11 (1943).
21. H. D. Papenfuss, J. F. Gross, M. Intaglietta and F. A. Treese, A transparent access chamber for the rat dorsal skin fold, *Microvasc. Res.* **18,** 311–318 (1979).
22. J. F. Gross, R. Roemer, M. Dewhirst and T. Meyer, A uniform thermal field in a hyperthermia chamber for microvascular studies, *Int. J. Heat Mass Transfer* **25,** 1313–1320 (1982).
23. M. W. Dewhirst, J. F. Gross and D. A. Sim, Effects of heating rate on normal and tumor microcirculatory function. In *Heat and Mass Transfer in the Microcirculation and Thermally Significant Vessels* (Edited by K. R. Diller and R. B. Roemer), pp. 73–78. ASME, New York (1986).
24. M. Taormina, K. R. Diller and C. R. Baxter, Burn induced alteration of vasoactivity in the cutaneous microcirculation. In *Heat and Mass Transfer in the Microcirculation and Thermally Significant Vessels* (Edited by K. R. Diller and R. B. Roemer), pp. 79–83. ASME, New York (1986).
25. S. J. Aggarwal, S. J. Shah, K. R. Diller and C. R. Baxter, Fluorescence digital microscopy of interstitial macromolecular diffusion in burn injury, *Comput. Biol. Med.* **19,** 245–261 (1989).
26. H. K. Yeung, S. J. Aggarwal, K. R. Diller and C. R. Baxter, Alteration of interstitial transport in the dermis following mild burns, *J. Burn Care Rehabil.* (in press).
27. L. J. Hayes, A users guide to PARAB: a two-dimensional linear time dependent finite element program, TICOM Rep #80-10, University of Texas (1980).
28. E. B. Becker, G. F. Carey and J. T. Oden, *Finite Elements: A First Course.* Prentice-Hall, New York (1981).
29. B. Fagrell, Microcirculation of the skin. In *The Physiology and Pharmacology of the Microcirculation* (Edited by N. A. Mortillaro), Vol. 2, pp. 133–180. Academic Press, New York (1984).
30. J. C. Chato, Heat transfer to blood vessels, *Trans. ASME, J. Biomech. Engr* **102,** 110–118 (1980).
31. A. D. M. Greenfield, The circulation through the skin. In *Handbook of Physiology, Circulation,* Vol. II, pp. 1325–1351. Williams & Wilkens, Baltimore (1963).
32. M. C. Conrad, *Functional Anatomy of the Circulation to the Lower Extremities.* Year Book Medical Publishers, Chicago (1971).
33. J. R. S. Hales, A. A. Fawcett, J. W. Bennett and A. D. Needham, Thermal control of blood flow through capillaries and arteriovenous anastomoses in skin of sheep, *Pflugers Archiv.* **378,** 55–63 (1978).
34. H. F. Bowman, E. G. Cravalho and M. Woods, Theory, measurement, and application of thermal properties of biomaterials, *Ann. Rev. Biophys. Bioengng* **4,** 43–80 (1975).
35. J. C. Chato, Measurement of thermal properties of biological materials. In *Heat Transfer in Medicine and Biology, Analysis and Applications* (Edited by A. Shitzer and R. C. Eberhart), Vol. 1, pp. 167–192. Plenum Press, New York (1985).
36. E. G. Cravalho, L. R. Fox and J. C. Kan, The application of the bioheat equation to the design of thermal protocols for local hyperthermia, *Ann. N.Y. Acad. Sci.* **335,** 86–97 (1980).
37. M. M. Chen, The tissue energy balance equation. In *Heat Transfer in Medicine and Biology, Analysis and Applications* (Edited by A. Shitzer and R. C. Eberhart), Vol. 1, pp. 153–166. Plenum Press, New York (1985).
38. S. Weinbaum and L. M. Jiji, A new simplified bioheat equation for the effect of blood flow on local average tissue temperature, *Trans. ASME, J. Biomech. Engr* **107,** 131–139 (1985).
39. W. J. Song, S. Weinbaum and L. M. Jiji, A theoretical model for peripheral tisue heat transfer using the bioheat equation of Weinbaum and Jiji, *Trans. ASME, J. Biomech. Engr* **109,** 72–78 (1987).
40. E. H. Wissler, Comments on the new bioheat equation proposed by Weinbaum and Jiji, *Trans. ASME, J. Biomech. Engr* **109,** 226–233 (1987).
41 S. Weinbaum and L. M. Jiji, Discussion of papers by Wissler and Baish *et al.* concerning the Weinbaum–Jiji bioheat equation, *Trans. ASME, J. Biomech. Engr* **109,** 234–237 (1987).

42. E. H. Wissler, Comments on Weinbaum and Jiji's discussion on their proposed bioheat equation, *Trans. ASME, J. Biomech. Engr* **109,** 355–356 (1987).
43. G. K. Blake, K. R. Diller and L. J. Hayes, Analysis of several models for simulating skin burns, *J. Burn Care Rehabil.* **12,** 177–189 (1991).
44. J. Bligh, Regulation of body temperature in man and other mammals. In *Heat Transfer in Medicine and Biology, Analysis and Applications* (Edited by A. Shitzer and R. C. Eberhart), Vol. 1, pp. 15–52. Plenum Press, New York (1985).
45. E. H. Wissler, Mathematical simulation of human thermal behavior using whole-body models. In *Heat Transfer in Medicine and Biology, Analysis and Applications* (Edited by A. Shitzer and R. C. Eberhart), Vol. 1, pp. 325–374. Plenum Press, New York (1985).

ANALYSE DE LESIONS DE TISSU PAR BRULURE: COMPARAISON DE MODELES DU CAS *IN SITU* ET D'UN MORCEAU DE PEAU

Résumé—Le champ de température variable dans la peau pendant une brûlure à la surface est modélisé par une technique aux éléments finis. Les deux systèmes physiques qui sont simulés sont le tissu *in situ* et un morceau de peau expérimental pour des études de brûlure. Les dégats locaux cumulés du tissu sont calculés en utilisant un modèle de type Arrhenius. L'analyse montre que les expériences de brûlure sur le morceau de peau à des températures supérieures à 70°C provoque des histoires thermiques qui sont très peu différentes de celles sur le tissu *in situ* pour des durées de brûlure inférieures à 15 s.

UNTERSUCHUNG DER GEWEBESCHÄDIGUNG BEI VERBRENNUNGEN: VERGLEICHENDE UNTERSUCHUNG AM TATSÄCHLICHEN GEWEBE UND AN MODELLEN VON HAUTSTÜCKCHEN

Zusammenfassung—Mit Hilfe der Finite-Elemente-Technik wird das zeitabhängige Temperaturfeld in der Haut während einer Oberflächenverbrennung modelliert. Die beiden simulierten physikalischen Systeme sind einerseits das tatsächliche Gewebe und andererseits eine Versuchskammer für Hautstückchen, welche für Verbrennungsuntersuchungen aufgebaut worden ist. Für die Berechnung konzentrierter Gewebeschädigungen wird das Schädigungsmodell nach Arrhenius verwendet. Die Berechnung zeigt, daß ein in der Versuchskammer bei Temperaturen bis zu 70°C durchgeführtes Verbrennungsexperiment bei Belastungsdauer unterhalb 15 s einen thermischen Verlauf ergibt, der sich nur geringfügig von demjenigen an tatsächlichem Gewebe unterscheidet.

АНАЛИЗ ПОВРЕЖДЕНИЙ ТКАНИ ПРИ ОЖОГЕ: СРАВНЕНИЕ МОДЕЛЕЙ ПЕРЕСАЖИВАЕМОЙ КОЖИ И *IN SITU*

Аннотация—С использованием метода конечных элементов моделируется нестационарное температурное поле, создаваемое в коже при поверхностном ожоге. Двумя моделируемыми физическими системами являются ткань *in situ* и в экспериментальном аппарате для пересадки кожи, применяемом при исследовании ожогов. Локальное кумулятивное повреждение в ткани рассчитывается при помощи модели повреждений типа Аррениуса. Анализ показывает, что термические истории, полученные при проведении экспериментов по ожогам в аппарате для пересадки кожи при температурах до 70°C, незначительно отличаются от полученных для ткани *in situ*, если продолжительность повреждающего действия составляет менее 15 секунд.